THE JOURNAL OF PHYSICAL CHEMISTRY B

Article

pubs.acs.org/JPCB

Base Triggered Enhancement of First Hyperpolarizability of a Keto−Enol Tautomer

Soumi De,[†] Manisha Ray,[†] Anusooya Y. Pati,[‡] and Puspendu K. Das[†,*]

[†]Department of Inorganic and Physical Chemistry, [‡]Solid State and Structural Chemistry Unit, Indian Institute of Science, Bangalore 560012, India

Supporting Information

ABSTRACT: This work describes the base triggered enhancement of first hyperpolarizability of a tautomeric organic molecule, namely, benzoylacetanilide (BA). We have used the hyper-Rayleigh scattering technique to measure the first hyperpolarizability (β) of BA which exists in the pure keto form in water and as a keto−enol tautomer in ethanol. Its anion exists in equilibrium with the keto and enol forms at pH 11 in aqueous solution. The β value of the anion form is 709×10^{-30} esu, whereas that of the enol is 232×10^{-30} esu and of the keto is 88×10^{-30} esu. There is an enhancement of β by ∼8 times for the anion and ∼3 times for the enol compared to the keto form. All these are achieved by altering the equilibrium between the three forms of BA by simple means. MP2 calculations reproduce the experimental trend, but the computed β values are much lower than the measured values. DFT calculations with the standard B3LYP functional could not predict the right order in the β values. The difference between experimental and calculated values is, perhaps, due to the fact that electron correlation effects are important in computing optical nonlinearities of large organic molecules and MP2 and B3LYP calculations done here for different forms of BA could not account for such effects adequately.

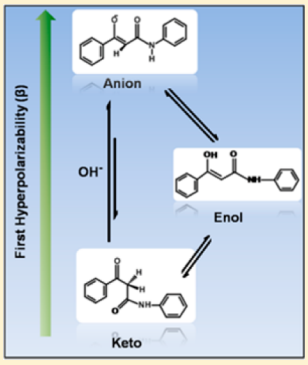

INTRODUCTION

Organic molecules possessing large quadratic nonlinear optical (NLO) coefficients have attracted considerable attention because of their application in electro-optic and optoelectronic devices. Various strategies have been adopted to produce organic molecules and materials with large first hyperpolarizability, high thermal stability, low photochemical degradability, and high transparency at telecommunication frequencies.[1,2] Molecules having large differences in their NLO property at various chemical or physical states are of potential interest for our ability to externally modulate the NLO effect in such nlophores. The change of state can be brought about by altering conditions in the environment such as changing the pH of the medium, by photochemical[3−6] and/or electrochemical[7,8] activation (switching). Generally the external stimulus alters the initial electronic configuration or geometry of the species significantly leading to a large change in the nonlinear coefficients. Several organic compounds such as azobenzene derivatives,[4,9] Schiff's bases,[10,11] and spiropyrans[12,13] exhibit this kind of structure−property relation under external stimulus.

Recently, Bogdan et al.[14] have combined hyper-Rayleigh scattering (HRS) experiments with quantum calculations and investigated solvent effects on the first hyperpolarizability (β) of the keto and enol forms of a *N*-(2-hydroxynapthylidene) aniline derivative. They reported larger β-value for the keto form ($\beta = 170 \times 10^{-30}$ esu) than the enol ($\beta = 34 \times 10^{-30}$ esu) form. The ratio of the keto to enol concentrations in the cyclohexane/ethanol binary mixture was tuned by changing the composition of the solvent mixture. The keto−enol equilibrium shifted toward the keto form with the increase in the proportion of ethanol in the binary mixture. As a consequence the polarity of the binary solvent mixture increased leading to a bathochromic shift of the absorption spectrum of the keto form and thus bringing in significant resonance contribution and enhancement in β. Density functional theory (DFT) calculations including solvent effects within the continuum model supported their experimental data. Sliwa et al.[15] studied two new anil molecules and switched their powder second harmonic generation (SHG) response by irradiation with UV light. Owing to an intramolecular enol-keto tautomerism the anil molecules exhibit modulated SHG response. The keto form of the anil showed three times higher SHG efficiency than the enol form. The second order nonlinearities of the enol and keto forms of two anil derivatives of salicylidene were calculated by Champagne et al.[16] in their molecular forms, unit cells as well as in their crystalline forms showing modest β values. Recently, several donor−acceptor substituted paracyclophane derived diketone compounds have been synthesized and their macroscopic NLO properties studied by both experiment and theory by Sergeeva et al.[17] Benzoylacetanilide (BA) is another 1,3-dicarbonyl compound which exists in a keto−enol equilibrium in a binary solvent mixture such as in water/ethanol[18] which has been studied in detail by Bishop et al.[19] In addition to the keto and enol forms, they pointed out that at an alkaline pH of 11, a third form which is the anionic form of BA exists in equilibrium with the keto and the enol forms (Scheme 1). At

Received: July 31, 2013

   dx.doi.org/10.1021/jp410368z | *J. Phys. Chem. B* XXXX, XXX, XXX−XXX

neutral pH, BA exists solely in the keto form and the equilibrium is shifted completely toward the keto side.

Scheme 1. Equilibrium among Three Different Forms of BA in Water, in Ethanol, and at pH 11

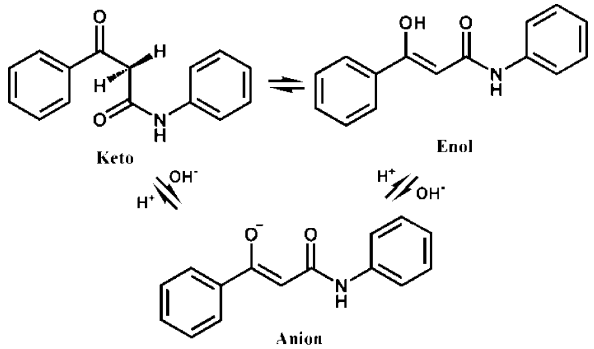

Sami et al.[20] studied the keto−enol equilibrium of several substituted BA molecules by UV and IR spectroscopy and reported the percent enol in ethanol solution. The percent of enol varies with the nature of the substitution on the phenyl ring directly attached to the keto group and the extent of enolization correlates with the Hammett σ-parameter of the substituent and follows Hammett equation closely. Therefore, BA is an ideal molecule to study the complex three-state keto−enol equilibrium by the HRS technique, where the contribution from the components can be varied either by changing the composition of the binary solvent mixture or by substitution in the phenyl ring attached directly to the keto side of BA. All the three forms have absorptions only in the ultraviolet and, therefore, resonance contribution to β in the visible and in the infrared is avoided unlike in keto−enol pairs where one or both the forms have absorption in the visible or near-infrared wavelengths. Apart from the intrinsic quadratic nonlinearity (β_0) of the keto and the enol forms, the possibility of realizing a large nonlinearity in BA is open since the anion which is stable under alkaline pH condition is likely to have a highly polarizable structure.

In this article, we present a detailed investigation on the first hyperpolarizability of different forms of BA. In the next section, we illustrate the experimental and theoretical methodology followed by results and discussion.

METHODOLOGY

A. Experiment. *UV−Vis Spectroscopy.* The UV−vis spectra of BA (Sigma-Aldrich) were recorded in Millipore water, ethanol (HPLC/spectroscopy grade), and water−ethanol mixture at different ratios as well as at pH 11 in a double beam UV spectrometer (Perkin-Elmer λ-750) with the excitation slit-width set at 2 nm. The anion of BA was prepared by adding a few drops of 6 M NaOH solution in 50 mL of an aqueous solution of BA until the pH reached 11 as monitored by a pH meter.

HRS Measurement. HRS measurements[21,22] were performed by using the fundamental wavelength (1064 nm) from a Q-switched Nd:YAG (INDI, Spectra-Physics, pulse width 10 ns and repetition rate 10 Hz) laser as the incident light source. The 1064 nm beam was focused by a 20 cm focal length plano-convex lens on a cylindrical sample cell (20 mL) after being guided by optics. The resulting incoherent second harmonic scattered light (532 nm) was collected at 90° by aspherical lens and allowed to fall on a photomultiplier tube (PMT) after passing through low band-pass and interference filters. The signal from the PMT was averaged over 512 shots, displayed on a digital storage oscilloscope and processed through a PC.

For a two component system of an analyte dissolved in a solvent, the intensity of the incoherently scattered second harmonic light ($I_{2\omega}$) follows

$$\frac{I_{2\omega}}{I_{\omega}^{2}} = G[N_{\text{Solvent}}\langle\beta_{\text{Solvent}}{}^{2}\rangle + N_{\text{Solute}}\langle\beta_{\text{Solute}}{}^{2}\rangle] \quad (1)$$

where I_ω is the intensity of the incident light, G is the instrument factor which accounts for scattering geometry, local field factors, etc., N_i's are the concentrations of the solvent and the solute, and β's are the first hyperpolarizabilities. The quadratic power dependence of the HRS signal intensity[23,24] with respect to the input laser light intensity (I_ω) was checked. The external reference method (ERM) was employed for β measurement of BA using *p*-nitroaniline (pNA) as the reference molecule. The β value of pNA in ethanol[25] was determined as 25.8×10^{-30} esu and the hyperpolarizabilties of all other molecules were measured against pNA in ethanol. Utilizing the slopes obtained by plotting normalized $I_{2\omega}$ vs N_{Solute} for BA and pNA in ethanol, β_{Solute} was determined from

$$\beta_{\text{Solute}} = \sqrt{\frac{(\text{slope})_{\text{Solute}}}{(\text{slope})_{\text{Reference}}}} \times \beta_{\text{Reference}} \quad (2)$$

B. Theoretical Calculation. We optimized the structures of the keto, enol, and anion forms of BA using Gaussian-09 suite of programs.[26] Both DFT and MP2 methods were employed in the calculation of β of the various forms of BA using the 6-31+G* basis set. Suponitsky et al.[27] reported the effect of basis sets on NLO properties of conjugated organic molecules and suggested that 6-31+G* basis set with hybrid density functionals are sufficient for qualitative agreement with experiment. Various basis sets and methods of calculation of hyperpolarizabilities of push−pull molecules were then compared by Wergifosse et al.[28] and others[29,30] and they all found that MP2 values are in much better agreement with experiments while DFT hybrid methods overestimate β values. BLYP, B3LYP, BHandHLYP functionals were used in a number of cases, but the trends in β values were not described well. We carried out geometry optimization, first hyperpolarizability and electronic excitation energy calculation of BA with B3LYP, CAM-B3LYP, and M052X exchange-correlation functionals. The best agreement with experiments in the excitation energies and gas phase β values was found with B3LYP functional only. To account for the solvent environment, we used the self-consistent reaction field (SCRF) model within the polarizable continuum model (PCM) for geometry optimization as well as for the calculation of hyperpolarizabilities. We carried out the calculation with water as the solvent for the keto and anion forms and ethanol for the enol. Frequency dependent hyperpolarizabilities (β_{1064}) were obtained with coupled perturbed Hartree−Fock method (CPHF) at experimental frequency (1.167 eV) by obtaining the first-order perturbation response vectors as described in the literature.[31−33] Static hyperpolarizabilities (β_0) were calculated from numerical derivative of energy. To find better agreement with experimental β values measured in solution, MP2 calculations within the SCRF model were done. The results obtained from B3LYP and MP2 calculations are reported here.

dx.doi.org/10.1021/jp410368z | J. Phys. Chem. B XXXX, XXX, XXX−XXX

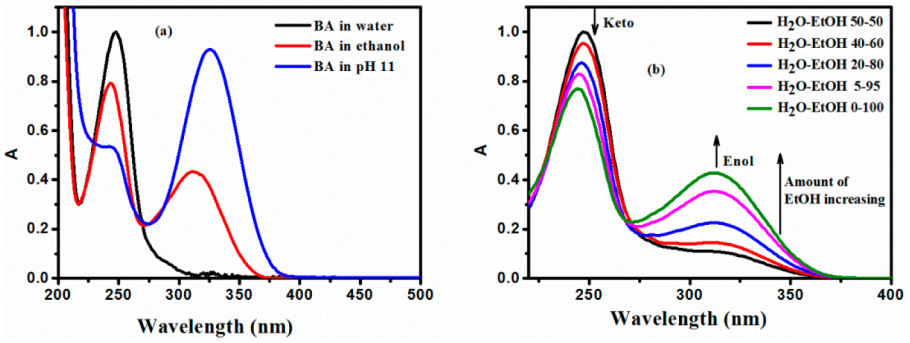

Figure 1. (a) Normalized UV–vis spectra of BA in three different solvents: in water (neutral pH), in ethanol, and at pH 11. (b) Variation of the normalized absorption spectra of BA as a function of water/ethanol binary mixture composition.

RESULTS AND DISCUSSION

UV–Vis Spectra. Figure 1a shows the UV–vis spectra of BA in three different solvents—Milli-Q water, ethanol and aqueous solution at pH 11. There is only one absorption peak of BA at 248 nm in water whereas two peaks appear in pure ethanol at 244 and 312 nm. At pH 11, BA shows a very distinct peak at 327 nm along with a small shoulder at ~244 nm. These bands were previously reported by Bishop et al.[19] and they assigned the 248 nm band of BA in pure water to the diketo form.

Two distinct bands at 244 and 312 nm in pure ethanol were assigned to the $\pi-\pi^*$ transitions centered on the ketonic carbonyl and the ethylenic (C═C) linkage, respectively.[20,34] The presence of two bands in ethanol provides evidence for the presence of both the keto and enol forms. In the anion form the shoulder originating from the ketonic carbonyl becomes small and the band originating from the C═C excitation shifts to the red.

The keto–enol tautomerism was examined by recording the change in absorption bands in water–ethanol binary solvent mixture. Figure 1b shows the change in absorption in the absorption spectra of BA (keto and enol bands) with the change in solvent composition. As we started increasing the amount of ethanol in the mixture, the band corresponding to the enol form began to appear slowly. In fact, it is clearly noticeable when the solvent composition reaches 50/50 [water (v)/ethanol (v)] ratio. The enol peak then grows steadily up to 100% ethanol. As the solvent polarity comes down with addition of ethanol, the enolic species in BA makes intramolecular H-bonding with the adjacent carbonyl group thus stabilizing the enol form in solution.

In order to get further insight into the problem, we carried out DFT and MP2 calculations on various forms of BA in the gas phase and in solution. The relative ground state energies of optimized structures (Figure 2) in water (for the keto and anionic forms) and in ethanol (for the enol form) are listed in Table 1. Because of the presence of the two CO groups, the molecule can be either in the *cis*- or in the *trans*-diketo conformations. We performed the calculations in both of these conformations for all the three forms. We noticed that the keto form in its *trans*-conformation is the most stable among all the three forms, both in the gas phase and in solution. The enol form can have two *cis*-conformations where either C7 (shown in Figure 2) or C9 undergoes enolization.[31] Since the former is more stable, for further investigation we have considered only the C7 enolized structure. The calculated bond-length of C7–C8 is 1.40 and 1.37 Å in the case of anion and enol, respectively

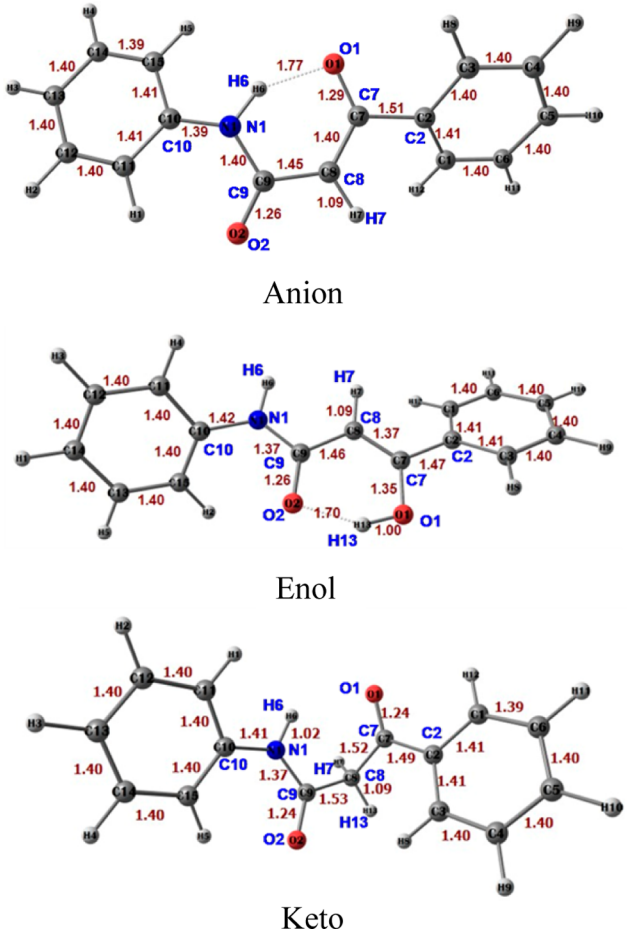

Figure 2. Optimized structures of BA in three different forms. Dark gray balls are C atoms, light gray balls are H atoms, red balls are O, and blue balls are N atoms.

Table 1. Calculated Ground State Energies of BA at the MP2 Level of Theory with 6-31+G* Basis Set (See Figure 2 for Numbering)

		in the gas phase (hartree)	in solution (hartree)
enol	C7-enolization	−782.2482	−782.2606
	C9-enolization	−782.2380	−782.2513
keto		−782.2573	−782.2679

and hence the structure resembles a C_6H_5–C═CH–CO–, a cinnamoyl moiety. On the other hand, for the keto form the C7–C8 bond length is 1.52 Å, a clear single bond and hence

dx.doi.org/10.1021/jp410368z | J. Phys. Chem. B XXXX, XXX, XXX–XXX

the structure is more like a benzoyl moiety. The details of the optimized structures are shown in the Supporting Information.

We calculated the vertical excitation energies and the corresponding transition dipole moments using TDDFT method. As seen from Table 2, the differences in energies of the relevant excited states with respect to the ground state from TDDFT calculations are comparable with experiment. For the anion and enol, there is a peak in the absorption spectrum above 300 nm which is dominated by the HOMO−LUMO transition. The relevant HOMO and LUMO of the enol and anion forms that are involved in the electronic transition above 300 nm are shown in Figure 3. In the anion and enol forms, the HOMO is delocalized over the hexagon formed by N1−H6−O1−C7−C8−C9 and O1−H13−O2−C9−C8−C7 atoms, respectively, whereas the LUMO is delocalized on the phenyl ring which is a part of the benzoyl moiety. The weaker transitions at 276 nm (dominated by HOMO to LUMO+3) and 282 nm (dominated by HOMO-1 to LUMO) for anion and enol, respectively, correspond to the electronic transition centered at the cinnamoyl moiety (see Supporting Information). Another weaker transition at 235 nm (HOMO-1 to LUMO+3) for the anion and at 247 nm (dominated by HOMO to LUMO+1 transition) for the enol correspond to the excitation of the benzoyl moiety (see Supporting Information). These two weaker transitions indicate the presence of both cinnamoyl and benzoyl characters in the enol and anion because similar transitions appear in cinnamic (285 nm) and benzoic (230 nm) acids, respectively. Since the keto form stabilizes in the trans-conformation, it does not form the hydrogen bond and the excitation is centered on the terminal benzoyl moieties (252 nm) dominated by HOMO-4 to LUMO transition, which is similar to the excitation in benzoic acid.

Table 2. Transition Wavelengths in nm of All Three Forms at the TDDFT Level of Theory[a]

form of BA	TDDFT	experiment
anion	348 (0.54)	325
	276 (0.15)	–
	235 (0.28)	244
enol	337 (0.95)	312
	282 (0.17)	–
	247 (0.17)	247
keto	252 (0.67)	248
	244 (0.24)	

[a]The numbers in brackets are oscillator strengths.

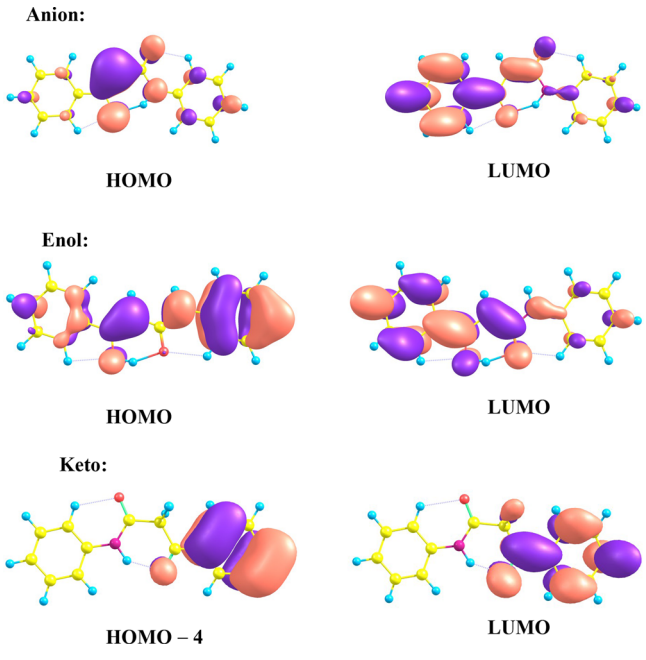

Figure 3. Relevant occupied and unoccupied molecular orbitals involved in the most prominent excitation for different forms of BA.

First Hyperpolarizability (β). The first hyperpolarizability of BA was determined in pure water at 10^{-4} - 10^{-5} M directly by using the slope obtained from the plot of $I_{2\omega}/I_{\omega}^{2}$ vs N_0 using the external reference method. This gives directly the β value of the keto form which is the only form that exists in pure water. But the enol and anion forms always stay in equilibrium with the keto form in ethanol and at pH 11 in water, respectively. Therefore, eq 1 which is valid for a pure analyte in a pure solvent has to be modified in the following manner for BA in ethanol.

$$\frac{I_{2\omega}}{I_{\omega}^{2}} = G[N_{\mathrm{EtOH}}\langle\beta_{\mathrm{EtOH}}{}^{2}\rangle + N_{\mathrm{keto}}\langle\beta_{\mathrm{keto}}{}^{2}\rangle + N_{\mathrm{enol}}\langle\beta_{\mathrm{enol}}{}^{2}\rangle] \tag{3}$$

At pH 11, eq 4 may be written as

$$\frac{I_{2\omega}}{I_{\omega}^{2}} = G[N_{\mathrm{H_2O}}\langle\beta_{\mathrm{H_2O}}{}^{2}\rangle + N_{\mathrm{keto}}\langle\beta_{\mathrm{keto}}{}^{2}\rangle + N_{\mathrm{anion}}\langle\beta_{\mathrm{anion}}{}^{2}\rangle] \tag{4}$$

As a result we collected the SHG signal ($I_{2\omega}$) from keto/enol and keto/anion species present in ethanol and water solutions, respectively. From normalized second harmonic signal intensity we obtained β_T's which is defined by the expression,

$$\frac{I_{2\omega}}{I_{\omega}^{2}} = G[N_{\mathrm{Solvent}}\langle\beta_{\mathrm{Solvent}}{}^{2}\rangle + N_0\langle\beta_T{}^{2}\rangle] \tag{5}$$

For BA in aqueous solution at pH 11, is written as

$$\langle\beta_T{}'^{2}\rangle = (1-\alpha')\langle\beta_{\mathrm{keto}}{}^{2}\rangle + \alpha'\langle\beta_{\mathrm{anion}}{}^{2}\rangle \tag{6}$$

while, in ethanol solution, we write

$$\langle\beta_T{}^{2}\rangle = (1-\alpha)\langle\beta_{\mathrm{keto}}{}^{2}\rangle + \alpha\langle\beta_{\mathrm{enol}}{}^{2}\rangle \tag{7}$$

where N_0 is the initial concentration of BA and α is the degree of conversion of the keto to the anion or to the enol forms as appropriate. We calculated α from the UV−vis absorption spectra showed in Figure 1, parts a and b. Figure 1b shows two bands in the UV−vis region in different H_2O−EtOH (v/v) mixtures. The band between 218 and 272 nm belongs to the keto form whereas the band at 273−382 nm belongs to the enol form of BA. We calculated the area under each band by fitting them with Gaussian curves and normalizing them with respect to the total area under the entire absorption curve. We have used eqs 8 and 9 for normalization of each band

$$A_{\mathrm{K}}\ (\%) = \frac{A_{\mathrm{K}}}{A_{\mathrm{T}}} \times 100 \tag{8}$$

$$A_{\mathrm{E}}\ (\%) = \frac{A_{\mathrm{E}}}{A_{\mathrm{T}}} \times 100 \tag{9}$$

dx.doi.org/10.1021/jp410368z | J. Phys. Chem. B XXXX, XXX, XXX−XXX

where A_T is the total area under the entire absorption curve. A_K (%) (218−272 nm) and A_E (%) (273−382 nm) are band areas for keto and enol forms, respectively.

The equilibrium constant (K_{eq}) for the keto−enol tautomeric equilibrium[35−38] is then calculated as

$$K_{eq} = -\frac{A_E\ (\%)}{A_K\ (\%)} \times \frac{\Delta A_K\ (\%)}{\Delta A_E\ (\%)} \qquad (10)$$

where ΔA_E (%) and ΔA_K(%) are percentile changes in respective band areas as a function of solvent composition. The equilibrium constant thus calculated vary within ±8%. From the equilibrium constant, the value of α was obtained which in turn gave us the concentrations of the keto and enol forms at each solvent composition. We first obtained β_T in 50/50 H_2O−EtOH (v/v) mixture and then obtained β_{enol} using the value of β_{keto} in water in eq 7 using the % keto form from the UV−vis spectral analysis described earlier. There will be a small difference in the value of β_{keto} in water and the same in water/ethanol mixture due to polarity change but it was neglected while calculating β_{enol} from eq 7. Similarly, we obtained β_{anion} from β_T at pH 11 utilizing eq 6. Figure 4 shows the HRS data as

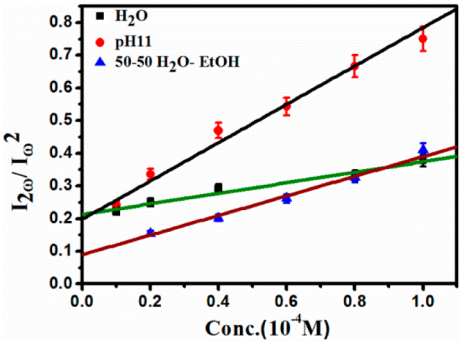

Figure 4. Normalized HRS plot for BA (a) in water, (b) in water at pH 11, and (c) in H_2O/EtOH (50/50). Experimental data points are fitted to straight lines.

a function of concentration of BA. The intrinsic hyperpolarizabilities of each form, β_0's were then calculated using the two-state model[39,40]

$$\frac{\beta}{\beta_0} = \frac{\lambda^4}{(\lambda^2 - 4\lambda_0^2)(\lambda^2 - \lambda_0^2)} \qquad (11)$$

where λ is the wavelength of incident light used in the experiment and λ_0 is the wavelength corresponding to the optical gap. The experimental β and β_0 values of each form are listed in Table 3 and as expected the resonance enhancement in β was not significant.

Computed static and frequency dependent β's are given in Table 4. Interestingly, although in the gas phase, B3LYP calculations follow qualitatively the experimental behavior, the same with solvent effects accounted through a dielectric continuum do not reflect the experimental trend. We then carried out MP2 calculations and obtained the frequency

Table 4. Calculated β Values from DFT (B3LYP) and MP2 Methods for the Keto, Enol, and Anion Forms of BA

	DFT calculation				MP2 calculation	
	gas		solution		gas	solution
	β_0	β_{1064}	β_0	β_{1064}	β_0	β_0
anion	9.4	44.7	2.3	11.7	7.9	14.1
enol	6.0	15.8	17.6	42.5	6.1	12.7
keto	3.6	3.7	8.4	8.0	2.5	6.8
$\beta_{enol}/\beta_{keto}$	1.7	4.3	2.1	5.3	2.4	1.9
$\beta_{anion}/\beta_{keto}$	2.6	12.1	0.3	1.5	3.2	2.1

independent β (which is β_0). The MP2 β_0 values reproduce the experimental trend qualitatively. In both the DFT and MP2 calculations, the keto form of BA has the lowest β value which is in agreement with experiment although the actual numbers are different. MP2 calculations yielded the highest β value for the anion, both in the gas phase and in solution which is in agreement with experiment. The highest β value exhibited by the anionic form of BA has been attributed to the presence of highly polarizable negative charge on the molecule. In calculations, ionic structures generally tend to show large errors in reproducing the experimental values.

The qualitative agreement of MP2 calculations with experiment clearly shows that calculations which handle correlation effects in a better way in such calculations are important in calculating β of large organic molecules. However, our calculated β values are not comparable quantitatively with experimental values due to the fact that MP2 calculation of static β is based on the finite field approach of calculation of nonlinearities. For calculation of β, third order derivatives of energy are needed. This implies calculation of energy values at four different electric field (small) values. Even at the MP2 levels of calculation, the energy values at finite electric field are not quantitatively accurate, as the calculations with electric field are carried out in the linear response regime. Frequency dependent β values can be calculated in a quantum sum-overstates method including full configuration interaction, which we have not performed here, since the system size is too big to carry out such calculations.

CONCLUDING REMARKS

In summary, we have demonstrated that BA in its keto and enol forms exhibit moderate hyperpolarizability in solution which increases by a factor of 8 with the addition of a base. The anion of the tautomer of BA is responsible for such enhancement which is achievable easily by manipulating the equilibrium among the different forms of BA. The experimental results have been supported, qualitatively, by calculations at the MP2 level but DFT calculation with B3LYP functional failed to reproduce the experimental trend indicating that electron correlation effects remain to be important in calculating second order nonlinearities of large organic molecules. But the MP2 calculations reproduce the experimental trends qualitatively although the actual experimental values of the first hyperpolarizability of BA in different forms do not match with MP2

Table 3. Experimental Hyperpolarizabilities of Three Forms of BA

	keto	enol	anion	$(\beta_{enol})_0/(\beta_{keto})_0$	$(\beta_{anion})_0/(\beta_{keto})_0$
β ($\times 10^{-30}$ esu)	88	232	709	2.6	8.1
β_0 ($\times 10^{-30}$ esu)	65	139	403	2.1	6.2

dx.doi.org/10.1021/jp410368z | J. Phys. Chem. B XXXX, XXX, XXX−XXX

values. This is, perhaps, due to the fact that electron correlation effects and solvation of these large organic moieties in polar solvents are not fully accounted for in the calculation. Sum-overstates model with full configuration interaction will probably account for the electron correlation effects in these molecules better but such calculations are beyond the scope of this work.

■ ASSOCIATED CONTENT

Supporting Information

Detailed description of the optimized geometry of three different forms and the relevant MO pictures. This material is available free of charge via the Internet at http://pubs.acs.org.

■ AUTHOR INFORMATION

Corresponding Author

*(P.K.D.) Telephone: 91-080-2293 2662 (Office). Fax: 91-080-23600683. E-mail: pkdas@ipc.iisc.ernet.in.

Notes

The authors declare no competing financial interest.

■ ACKNOWLEDGMENTS

We thank Prof. S. Ramasesha for many helpful discussions. YAP would like to thank DST, Govt. of India for financial support.

■ REFERENCES

(1) Dalton, L. R.; Sullivan, P. A.; Bale, D. H. Electric Field Poled Organic Electro-optic Materials: State of the Art and Future Prospects. *Chem. Rev.* **2010**, *110*, 25−55.

(2) Blanchard-Desce, M.; Alain, V.; Bedworth, P. V.; Marder, S. R.; Fort, A.; Runser, C.; Barzoukas, M.; Lebus, S.; Wortmann, R. Large Quadratic Hyperpolarizabilities with Donor-Acceptor Polyenes Exhibiting Optimum Bond Length Alternation: Correlation between Structure and Hyperpolarizability. *Chem.—Eur. J.* **1997**, *3*, 1091−1104.

(3) Nitadori, H.; Ordronneau, L.; Boixel, J.; Jacquemin, D.; Boucekkine, A.; Singh, A.; Akita, M.; Ledoux, I.; Guerchaisa, V.; Bozec, H. L. Photoswitching of the Second-Order Nonlinearity of a Tetrahedral Octupolar Multi DTE-Based Copper(I) Complex. *Chem. Commun.* **2012**, *48*, 10395−10397.

(4) Loucif-Saibi, R.; Nakatani, K.; Delaire, J. A.; Dumont, M.; Sekkat, Z. Photoisomerization and Second Harmonic Generation in Disperse Red One-Doped and -Functionalized Poly(methy1 methacrylate) Films. *Chem. Mater.* **1993**, *5*, 229−236.

(5) Coe, B. Molecular Materials Possessing Switchable Quadratic Nonlinear Optical Properties. *Chem.—Eur. J.* **1999**, *5*, 2464−2471.

(6) Mancois, F.; Sanguinet, L.; Pozzo, J.-L.; Guillaume, M.; Champagne, B.; Rodriguez, V.; Adamietz, F.; Ducasse, L.; Castet, F. Acido-Triggered Nonlinear Optical Switches: Benzazolo-Oxazolidines. *J. Phys. Chem. B* **2007**, *111*, 9795−9802.

(7) Coe, B. Switchable Nonlinear Optical Metallochromophores with Pyridinium Electron Acceptor Groups. *Acc. Chem. Res.* **2006**, *39*, 383−393.

(8) Kaur, P.; Kaur, M.; Depotter, G.; Cleuvenbergen, S. V.; Asselberghs, I.; Clays, K.; Singh, K. Thermally Stable Ferrocenyl "Push−Pull" Chromophores with Tailorable and Switchable Second-Order Non-Linear Optical Response: Synthesis and Structure−Property Relationship. *J. Mater. Chem.* **2012**, *22*, 10597−10608.

(9) Atassi, Y.; Chauvin, J.; Delaire, J. A.; Delouis, J.; Fanton-Maltey, I.; Nakatani, K. Photoinduced Manipulations of Photochromes in Polymers: Anisotropy, Modulation of the NLO Properties and Creation of Surface Gratings. *Pure Appl. Chem.* **1998**, *70*, 2157−2166.

(10) Plaquet, A.; Guillaume, M.; Champagne, B.; Rougier, L.; Mancüois, F.; Rodriguez, V.; Pozzo, J.; Ducasse, L.; Castet, F. Investigation on the Second-Order Nonlinear Optical Responses in the Keto-Enol Equilibrium of Anil Derivatives. *J. Phys. Chem. C* **2008**, *112*, 5638−5645.

(11) Antonov, L.; Fabian, W. M. F.; Nedeltcheva, D.; Kamounah, F. S. Tautomerism of 2-Hydroxynaphthaldehyde Schiff Bases. *J. Chem. Soc,. Perkin Trans.* **2000**, *2*, 1173−1179.

(12) Atassi, Y.; Delaire, J. A.; Nakatani, K. Coupling between Photochromism and Second-Harmonic Generation in Spiropyran- and Spirooxazine-Doped Polymer Films. *J. Phys. Chem.* **1995**, *99*, 16320−16326.

(13) Berkovic, G.; Krongauz, V.; Weiss, V. Spiropyrans and Spirooxazines for Memories and Switches. *Chem. Rev.* **2000**, *100*, 1741−1753.

(14) Bogdan, E.; Plaquet, A.; Antonov, L.; Rodriguez, V.; Ducasse, L.; Champagne, B.; Castet, F. Solvent Effects on the Second-Order Nonlinear Optical Responses in the Keto-Enol Equilibrium of a 2-Hydroxy-1-naphthaldehyde Derivative. *J. Phys. Chem. C* **2010**, *114*, 12760−12768.

(15) Sliwa, M.; Letard, S.; Malfant, I.; Nierlich, M.; Lacroix, P. G.; Asahi, T.; Masuhara, H.; Yu, P.; Nakatani, K. Design, Synthesis, Structural and Nonlinear Optical Properties of Photochromic Crystals: Toward Reversible Molecular Switches. *Chem. Mater.* **2005**, *17*, 4727−4735.

(16) Segerie, A.; Castet, F.; Kanoun, M. B.; Plaquet, A.; Liegeois, V.; Champagne, B. Nonlinear Optical Switching Behavior in the Solid State: A Theoretical Investigation on Anils. *Chem. Mater.* **2011**, *23*, 3993−4001.

(17) Sergeeva, E. V.; Puntus, L. N.; Kajzar, F.; Rau, I.; Sahraoui, B.; Pekareva, I. S.; Suponitsky, K. Y.; Bushmarinov, I. S.; Lyssenko, K. A. Keto-Enol Tautomerism and Nonlinear Optical Properties in β-diketones Containing [2.2]Paracyclophane. *Opt. Mater.* **2013**, *36*, 47−52.

(18) Reichardt, C. *Solvent and Solvent Effects in Organic Chemistry*, Third Updated and Enlarged ed; WILEY-VCH Verlag GmbH & Co. KGaA: Weinheim; Germany, 2002.

(19) Bishop, C.; Tong, L. K. J. The Kinetics of the Keto-Enol Tautomerism of Benzoylacetanilide. *J. Phys. Chem.* **1962**, *66*, 1034−1040.

(20) Sami, A.; Shawali, A. S.; Naoum, M. M.; Ibrahim, S. A. Spectra and Keto-Enol Equilibrium of Benzoylacetanilides. *Bull. Chem. Soc. Jpn.* **1972**, *45*, 2504−2507.

(21) Clays, K.; Persoons, A. Hyper-Rayleigh Scattering in Solution. *Phys. Rev. Lett.* **1991**, *66*, 2980−2983.

(22) Clays, K.; Persoons, A. Hyper-Rayleigh Scattering in Solution. *Rev. Sci. Instrum.* **1992**, *63*, 3285−3289.

(23) Kodaira, T.; Watanabe, A.; Ito, O.; Matsuda, M.; Clays, K. Hyper-Rayleigh Scattering Studies of an Ionic Species Solvent Effect on Hyperpolarizability of 1-Anilinonaphthalene-8-Sulfonic Acid Ammonium Salt. *J. Chem. Soc. Faraday Trans.* **1997**, *93*, 3039−3044.

(24) Pauley, M. A.; Guan, H. W.; Wang, C. H.; Jen, A. K. Y. Determination of First Hyperpolarizability of Nonlinear Optical Chromophores by Second Harmonic Scattering Using an External Reference. *J. Chem. Phys.* **1996**, *104*, 7821−7829.

(25) Huyskens, F. L.; Huyskens, P. L.; Persoons, A. P. Solvent Dependence of the First Hyperpolarizability of p-Nitroanilines: Differences between Nonspecific Dipole−Dipole Interactions and Solute−Solvent H-Bonds. *J. Chem. Phys.* **1998**, *108*, 8161−8171.

(26) Frisch, M. J.; Trucks, G. W.; Schlegel, H. B.; Scuseria, G. E.; Robb, M. A.; Cheeseman, J. R.; Scalmani, G.; Barone, V.; Mennucci, B.; Petersson, G. A. et al. *Gaussian 2009*, Revision A.1, Gaussian, Inc.: Wallingford CT, 2009.

(27) Suponitsky, K. Y.; Tafur, S.; Masunov, A. E. Applicability of Hybrid Density Functional Theory Methods to Calculation of Molecular Hyperpolarizability. *J. Chem. Phys.* **2008**, *129*, 044109 1−11.

(28) Wergifosse, M.; Champagne, B. Electron Correlation Effects on the First Hyperpolarizability of Push−Pull π-Conjugated Systems. *J. Chem. Phys.* **2011**, *134*, 074113 1−13.

(29) Torrent-Sucarrat, M.; Sola, M.; Duran, M.; Luis, J. M.; Kirtman, B. Basis Set and Electron Correlation Effects on Ab Initio Electronic and Vibrational Nonlinear Optical Properties of Conjugated Organic Molecules. *J. Chem. Phys.* **2003**, *118*, 711−718.

(30) Skwara, B.; Bartkowiak, W.; Zawada, A.; Gora, R. W.; Leszczynski, J. On the Cooperativity of the Interaction-Induced (Hyper)polarizabilities of the Selected Hydrogen-bonded Trimers. *Chem. Phys. Lett.* **2007**, *436*, 116−123.
(31) Sekino, H.; Bartlett, R. J. Frequency Dependent Nonlinear Optical Properties of Molecules. *J. Chem. Phys.* **1986**, *85*, 976−989.
(32) Rice, J. E.; Amos, R. D.; Colwell, S. M.; Handy, N. C.; Sanz, J. Frequency Dependent Hyperpolarizabilities with Application to Formaldehyde and Methyl fluoride. *J. Chem. Phys.* **1990**, *93*, 8828−8839.
(33) Rice, J. E.; Handy, N. C. The Calculation of Frequency-Dependent Hyperpolarizabilities Including Electron Correlation Effects. *Int. J. Quantum Chem.* **1992**, *43*, 91−118.
(34) Lowe, J. U., Jr.; Ferguson, L. N. The Direction of Enolization of Benzoylacetones. *J. Org. Chem.* **1965**, *30*, 3000−3003.
(35) Antonov, L.; Nedeltcheva, D. Resolution of Overlapping UV−Vis Absorption Bands and Quantitative Analysis. *Chem. Soc. Rev.* **2000**, *29*, 217−227.
(36) Antonov, L.; Petrov, V. Quantitative Analysis of Undefined Mixtures−"Fishing Net" Algorithm. *Anal. Bioanal. Chem.* **2002**, *374*, 1312−1317.
(37) Nishimura, N.; Danjo, K.; Sueishi, Y.; Yamamoto, S. Solvent and Pressure Effects on the Tautomeric Equilibrium of 4-Phenylazo-1-naphthol. *Aust. J. Chem.* **1988**, *41*, 863−872.
(38) Metzler, D. E.; Harris, C. M.; Johnson, R. J.; Saino, D. B.; Thomson, J. A. Spectra of 3-Hydroxypyridines. Band-Shape Analysis and Evaluation of Tautomeric Equilibria. *Biochemistry* **1973**, *12*, 5377−5392.
(39) Oudar, J. L.; Chemla, D. S. Hyperpolarizabilities of the Nitroanilines and Their Relations to the Excited State Dipole Moment. *J. Chem. Phys.* **1977**, *66*, 2664−2668.
(40) Marder, S. R.; Kippelen, B.; Jen, A K.-Y.; Peyghambarian, N. Design and Synthesis of Chromophores and Polymers for Electro-Optic and Photorefractive Applications. *Nature* **1997**, *388*, 845−851.